Brain (1998), **121,** 1749–1758

Reciprocal inhibitory visual–vestibular interaction
Visual motion stimulation deactivates the parieto-insular vestibular cortex

Thomas Brandt,[1] Peter Bartenstein,[2] Anika Janek[2] and Marianne Dieterich[1]

[1]*Department of Neurology, Ludwig-Maximilians-University, Klinikum Grosshadern and* [2]*Department of Nuclear Medicine, Technical University, Munich, Germany*

Correspondence to: Thomas Brandt, MD, Department of Neurology, Klinikum Grosshadern, Ludwig-Maximilians-University, Marchioninistrasse 15, 81377 Munich, Germany

Summary
The vestibular system—a sensor of head accelerations—cannot detect self-motion at constant velocity and thus requires supplementary visual information. The perception of self-motion during constant velocity movement is completely dependent on visually induced vection. This can be linear vection or circular vection (CV). CV is induced by large-field visual motion stimulation during which the stationary subject perceives the moving surroundings as being stable and himself as being moved. To determine the unknown cortical visual–vestibular interaction during CV, we conducted a PET activation study on CV in 10 human volunteers. The PET images of cortical areas activated during visual motion stimulation without CV were compared with those with CV. Hitherto, CV was explained neurophysiologically by visual–vestibular convergence with activation of the vestibular nuclei, thalamic subnuclei and vestibular cortex. If CV were mediated by the vestibular cortex, one would expect that an adequate visual motion stimulus would activate both the visual and vestibular cortex. Contrary to this expectation, it was shown for the first time that visual motion stimulation with CV not only activates a medial parieto-occipital visual area bilaterally, separate from middle temporal/medial superior temporal areas, it also simultaneously deactivates the parieto-insular vestibular cortex. There was a positive correlation between the perceived intensity of CV and relative changes in regional CBF in parietal and occipital areas. These findings support a new functional interpretation: reciprocal inhibitory visual–vestibular interaction as a multisensory mechanism for self-motion perception. Inhibitory visual–vestibular interaction might protect visual perception of self-motion from potential vestibular mismatches caused by involuntary head accelerations during locomotion, and this would allow the dominant sensorial weight during self-motion perception to shift from one sensory modality to the other.

Keywords: PET activation study; self-motion perception; vestibular cortex; visual cortex; circular vection

Abbreviations: BA = Brodmann area; CV = circular vection; rCBF = regional cerebral blood flow

Introduction
Vestibular stimuli invariably lead to the sensation of body motion. Stimuli of visual motion, however, can always have two perceptual interpretations: either self-motion or object-motion (Brandt *et al*., 1973). The subject who observes moving stimuli may perceive either himself as being a stationary observer of external movement (egocentric motion perception) or a moving observer of a stationary surround. The sensation of apparent self-motion during large-field visual motion stimulation [circular vection (CV)] is a common visual perception, from which neurophysiological inferences about visual–vestibular interaction can be drawn (Dichgans and Brandt, 1978). Visual self-motion can be perceived while gazing at moving clouds, or a train moving on the adjacent track in a train station. CV is not merely an insignificant visual illusion, but an essential mechanism for adequate perception of self-motion in order to control postural balance and to guide vehicles, especially at constant velocity. Vestibular information about motion is elicited only through acceleration or deceleration; it ceases when the cupulae within the semicircular canals or the otoliths have returned to their resting position during constant velocity. Our perception of self-motion during constant velocity car motion is completely dependent on visually induced vection.

It is not known which cortical areas are involved in the visual perception of self-motion. Is it the visual cortex, the vestibular cortex or both, or perhaps a third totally separate area? If CV is mediated by the vestibular cortex, an adequate visual motion stimulus should activate this area. If CV is

mediated by the visual cortex, then areas close to the motion-sensitive middle temporal (or V5) and medial superior temporal areas (or V5A) should be activated. A third and most interesting alternative would be a reciprocal activation–deactivation of visual and vestibular cortical areas during CV. Consideration of this alternative is based on our recent human PET study in which a significant deactivation of the visual cortex was found during vestibular (caloric) stimulation (Wenzel *et al.*, 1996). An inhibitory reciprocal interaction during CV at first glance appears paradoxical. However, closer examination suggests that it would be functionally useful, especially during passive transportation in vehicles, when there are contradictory visual and vestibular inputs.

We addressed these questions in a PET activation/deactivation study on visual self-motion perception, in which cerebral blood flow (CBF) was repeatedly measured by an $H_2{}^{15}O$-bolus technique and visual motion stimulation in healthy volunteers wearing goggles especially designed for such stimulation. The experimental paradigm was to compare cerebral activation during visual motion stimulation with CV and without apparent self-motion. If the activated (or deactivated) areas during visual motion stimulation without concurrent CV are compared with those activated during visual motion stimulation with concurrent CV, the differential areas should indicate the cerebral loci that are critical for determining whether visual motion is perceived as self-motion or object-motion.

Methods

Subjects

Ten healthy right-handed volunteers, aged 26–49 years (mean age 37.2 years; two females and eight males), participated in the study, after giving their informed written consent in accordance with the Helsinki Declaration. The study was approved by the Ethics Committee of the Technical University, Munich, as well as the radiation protection authorities.

Visual motion stimulation

Stimulation was performed with the subjects in supine position and wearing a helmet in which a display was mounted with the field of visual motion stimulation subtending 40° in horizontal and vertical dimensions. Four conditions were presented to the subjects, who were instructed to stare at the grey centre during the stimulus presentation without fixating any individual structure and without following the dots with their eyes. Condition A consisted of a light grey background with a central circle in a darker shade of grey (baseline). Condition B had the same background and central circle, but the presentation included a total of 190 red and black dots of various sizes (1/40–1/100 of the screen size), randomly distributed in the field of view, and moving in random order at the same speed as in conditions C and D. This visual motion stimulation did not induce any apparent self-motion (no CV). Condition C was identical to condition B but with the difference that all dots rotated counter-clockwise at a constant angular velocity of 40°/s. This condition induced an apparent self-motion in all subjects (clockwise CV) in the roll plane which was opposite in direction to that of the moving dots, i.e. clockwise. Condition D was identical to condition C, but with the sole difference that the dots rotated clockwise. This condition also induced apparent self-motion (counter-clockwise CV) in all subjects.

Subjects rated the intensity of CV by assigning arbitrary values (from 1 to 5) to each condition. To avoid additional uncontrollable motor and attentional components in the paradigms, rating CV intensity and checking whether and when the subjects entered vection during the scan were restricted to interviews between the scans. Thanks to careful subject selection and previous training, all subjects experienced vection during the scanning periods when conditions C and D were presented and no scans had to be omitted. The subjects were selected so that all entered vection within 30 s after onset of the stimulus. It was not possible to record torsional eye movements during stimulation in the PET scanner because of the configuration of the helmet. Therefore, three-dimensional video-oculographic recordings were made in three of the 10 subjects when they were exposed to the same stimulus pattern under laboratory conditions but without wearing the helmet. The irregular rotatory nystagmus beats recorded in this way exhibited a maximum frequency of 0.5–2 Hz with a maximum amplitude of 0.5–3° and a maximum slow phase velocity of 1–8°/s for both stimulus directions.

PET: scanning and data acquisition

Measurements were made with a Siemens 951 R/31 PET scanner (CTI, Knoxville, Tenn., USA) in 3D mode with a total axial field of view of 10.5 cm and no interplane dead space. Attenuation was corrected using a transmission scan with an external $^{68}Ge/^{68}Ga$ ring source obtained prior to the tracer injection. Twelve PET image sets were obtained for each subject under the four above-mentioned conditions. Each condition was presented three times in random order. Each stimulus presentation began simultaneously with tracer administration and continued until the end of acquisition. An infusion pump was used to administer a dose of 7.5 mCi $H_2{}^{15}O$ intravenously over 30 s with a semibolus injection. Single frames were acquired for 50 s after the tracer appeared in the brain. To allow for decay of activity, and to avoid after-effects and motion sickness, the interval between the acquisitions was 10 min.

Image analysis

Images were analysed on a SPARC 10 workstation (Sun Microsystems) using commercial interactive image display software. After corrections were made for randoms, dead

time and scatter, images were reconstructed by filtered back-projection with a Hanning filter (cut-off frequency 0.4 cycles per projection element). This yielded 31 slices with a 128×128 pixel matrix (pixel size 2.0 mm) and interplane separation of 3.375 mm.

Tracer counts were proportionally normalized to the global cerebral activity (Fox and Raichle, 1984), which was arbitrarily set at 1000 in order to determine relative tissue activity. An automated program was used to coregister, reslice and transform the image arrays into the stereotactic space of Talairach (Talairach and Tournoux, 1988) as described previously (Minoshima *et al*., 1993, 1994). To eliminate individual differences in gyral anatomy, these images were further smoothed with a three-dimensional Gaussian filter, giving an effective resolution of ~17 mm (full width half maximum). Differences between the control and activation images, each initially averaged within subjects, were expressed as voxel-by-voxel *t*-values using a pooled variance estimated from the whole-brain grey matter (Worsley *et al*., 1992). Since the resulting *t*-map is known to approximate closely a standard Gaussian distribution (Worsley *et al*., 1992), these values were described as *Z*-scores. To determine a threshold for significant activation on the resulting *t*-map, we calculated the image smoothness (Friston *et al*., 1991) and estimated a statistical threshold at one-tail (positive) probability of $P = 0.05$ using a statistical model that adjusts multiple comparisons and inherent correlation of neighbouring pixels (Worsley *et al*., 1992). For the areas attributed to visual and vestibular functions for which we had a theory-driven, a priori hypothesis, a *Z*-score of >3 in the respective regions was considered representative of a significant change (increase or decrease) in regional CBF (rCBF). This corresponds to *t*-values that, without correction for multiple comparisons, achieve a probability of $P < 0.001$ (Kosslyn *et al*., 1994).

For the quantitative analysis of rCBF changes we defined three-dimensional templates covering the voxels, in which activation in the subjects reached a *Z*-score of >0.05 when not corrected for multiple comparisons in the respective areas, and we calculated the mean relative rCBF changes in these areas (Wenzel *et al*., 1996; Bartenstein *et al*., 1997).

To assess the effect of the perceived intensity of CV on the areas activated by the stimuli inducing CV, Pearson's linear correlation was performed on a pixel-by-pixel basis. The rCBF increases for this correlation were determined by comparing conditions C and D with the baseline condition A. The correlation coefficient was used, after Fisher's transformation, to calculate the *Z*-values (Bartenstein *et al*., 1997). For the statistical comparison, a correlation coefficient of >0.70 was considered significant (approximately equivalent to $P < 0.05$). In addition, the rCBF increases of the medial parieto-occipital cortex and of the primary visual cortex induced by the clockwise and counter-clockwise CV conditions compared with baseline (condition A) were correlated with decreases in rCBF in the posterior insula induced by these conditions using the same statistical methods. The rCBF changes were determined from the above-described templates covering the respective areas.

Results

Cortical areas activated/deactivated during apparent self-motion

Statistical subtraction analysis (A versus B, i.e. grey background versus randomly moving dots) revealed a nearly symmetrical, highly significant increase of rCBF over extensive areas of the occipital cortex corresponding to Brodmann areas (BA) 17, 18 and 19. Talairach coordinates of the voxels with the most significant increases were as follows: $x, y, z = -8, -73, 2$ ($Z = 8.71$) for the right side and $x, y, z = 17, -85, 16$ ($Z = 7.29$) for the left side. In addition, the moving dots induced a statistically significant increase in rCBF [above the estimated *Z*-threshold of 4.36 ($P < 0.05$) corrected for multiple comparisons in smaller areas] in both temporal lobes (right BA 37, with $Z = 5.76$ at $x, y, z = -46, -73, 2$, and left BA 37, with $Z = 5.66$ at $x, y, z = 44, -73, 0$) and in the frontal cortex (left BA 47, with $Z = 4.41$ at $x, y, z = 39, 28, -9$). None of the subjects experienced any CV under conditions A or B. Stimulus conditions C and D (clockwise and counter-clockwise rotations) always resulted in perceived self-motion (CV) in the direction opposite to that of the moving dots. The intensity of CV assigned by the subjects ranged from 1 to 4 for condition C (mean 2.6) and from 2 to 4.5 for condition D (mean 2.9). Visual motion stimulation did not induce motion sickness in any subject.

A comparison of conditions C (clockwise CV) and B (random movement and no CV) using statistical subtraction analysis revealed a bilateral increase in rCBF in the precuneus and the adjacent parts of the occipital and parietal cortex (Table 1). A comparison of the conditions C (clockwise CV) and B (random movement and no CV) revealed a mean relative increase in rCBF in this region of 6.1%. Comparison of conditions C (clockwise CV) and A (baseline) showed a 6.7% rCBF increase. Comparison of conditions C and B revealed an additional small area of activation in the right parahippocampal gyrus.

Areas that did not directly process visual or vestibular information but where the activation reached a *Z*-score of >3 were located in the posterior cingulate (right BA 24, with $Z = 4.35$ at $x, y, z = -3, -17, 40$) and left prefrontal cortex (BA 46, with $Z = 3.00$ at $x, y, z = 46, -21, 25$).

Comparison of condition D (counter-clockwise CV) with B (no CV) again revealed bilateral activation of the medial parieto-occipital areas (Table 2 and Fig. 1). Here the mean relative increase in rCBF was 4.9%. Comparison of conditions D and A (baseline) showed a 9.4% increase in rCBF. An additional activation of an area linked to brainstem/midbrain structures was observed during this comparison as was frontal activation (left BA10/46, with $Z = 3.27$ at $x, y, z = 28, 55, 7$, and right BA 9, with $Z = 3.27$ at $x, y, z = -21, 44, 34$).

Table 1 *Increased rCBF under condition C (clockwise CV) compared with condition B (random movement)*

Areas	*x*	*y*	*z*	*Z*-score	*P*-value
BA 30, right parahippocampal gyrus	–10	–42	–7	4.35	<0.000001
BA 7/18/19/31, left parieto-occipital	1	–82	25	3.74	<0.00001
BA 7/19/31 right parieto-occipital	–6	–31	43	3.20	<0.001

Coordinates *x*, *y* and *z* as in Talairach and Tournoux (1988).

Table 2 *Increased rCBF under condition D (counter-clockwise CV) compared with condition B (random movement)*

Areas	*x*	*y*	*z*	*Z*-score	*P*-value
BA 7/18/19/31, left parieto-occipital	6	–82	27	4.05	<0.0001
BA 7/18/19/31, right parieto-occipital	–8	–64	18	3.63	<0.001
Left midbrain	12	–26	–11	3.30	<0.001

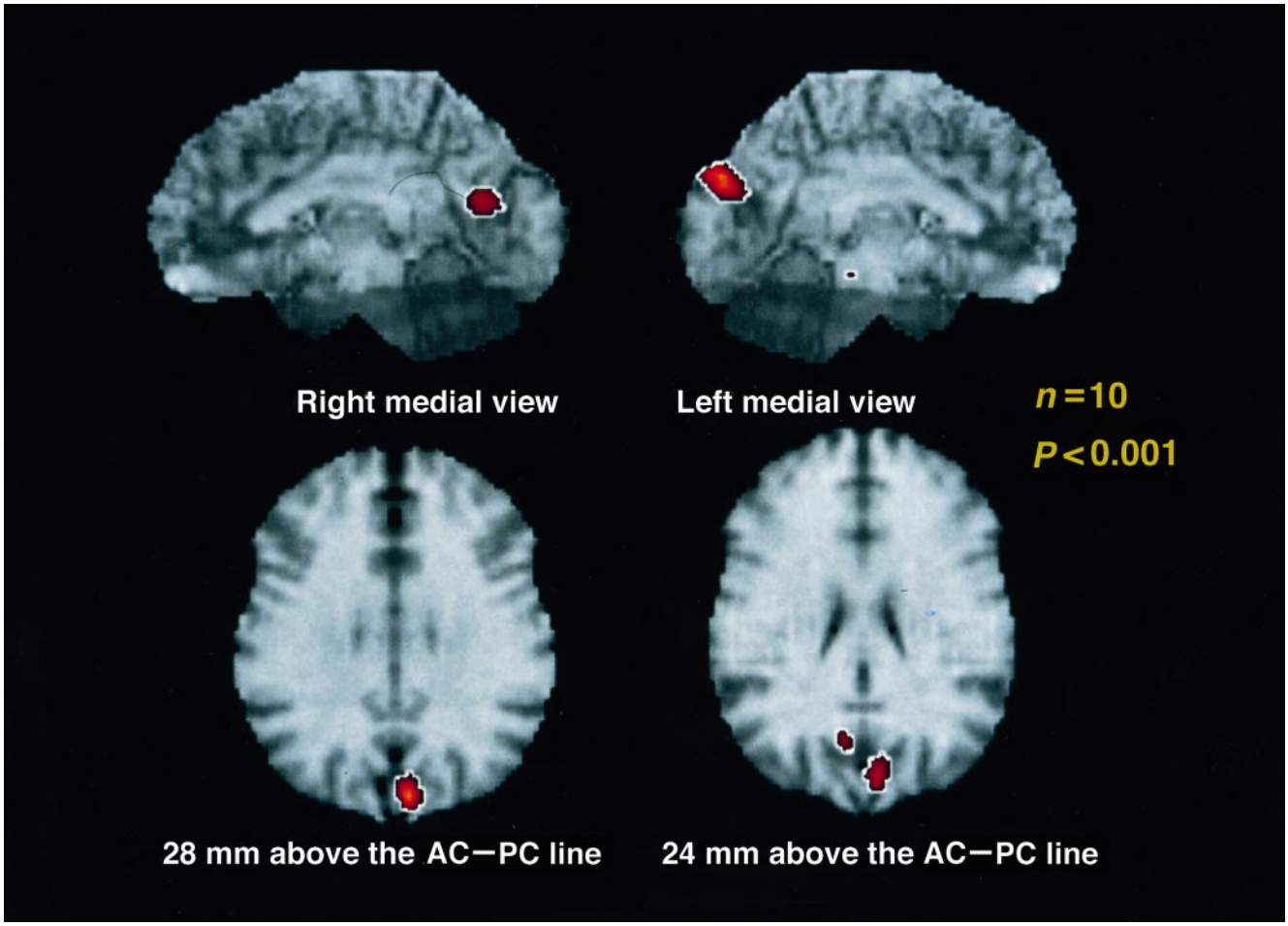

Fig. 1 Comparison of the relative rCBF increase under condition D, which induced CV (counter-clockwise), with the control condition B (random movement). All voxels with significant flow above the statistical threshold ($P < 0.001$, corrected for multiple comparisons) are shown. The medial views and transverse images illustrate the selective bilateral activation of areas at the border between occipital and parietal cortex.

Posterior cingulate activation ($x, y, z = –1, –17, 43$) reached a significance level of only $P < 0.004$ ($Z = 2.7$).

Statistical subtraction analysis (B versus C) showed a significant bilateral decrease in the posterior part of the insula (Tables 3 and 4). This was not simply lack of activation in condition C but reflected a real deactivation (‘inhibition’?)

Table 3 *Decreased rCBF under condition C (clockwise CV) compared with condition B (random movement)*

Areas	*x*	*y*	*z*	*Z*-score	*P*-value
BA 19, left occipital (V5)	48	–78	–4	4.51	<0.00001
BA 28, left parahippocampal gyrus	21	–19	–9	3.77	<0.00001
BA 19, right occipital (V5)	–48	–71	–4	3.55	<0.001
BA 22/42, right superior temporal	–55	–26	14	3.46	<0.001
BA 18, right occipital	–15	–71	–2	3.45	<0.001
Left posterior insula	35	–33	–4	3.32	<0.001
BA 21/37, right inferior temporal	–48	–42	–9	3.17	<0.001
Right thalamus	–17	–22	–2	3.12	<0.001

Table 4 *Decreased rCBF under condition D (counter-clockwise CV) compared with condition B (random movement)*

Area	*x*	*y*	*z*	*Z*-score	*P*-value
Right posterior insula	–30	–8	2	3.35	<0.001
BA 19, left occipital (V5)	48	–78	–4	3.28	<0.001
Left posterior insula	30	–28	–2	3.17	<0.001
BA 18, right occipital	–26	–94	–10	3.15	<0.001
BA 19, right occipital (V5)	–46	–76	–2	3.00	<0.001

of this area when visual motion stimulation induced CV. Comparison of conditions C (clockwise CV) and B (no CV) revealed a mean relative decrease in the left posterior insula of –6.8%. The corresponding value for the right posterior insula was –2.4%. Comparison with the baseline condition A showed a decrease of the left posterior insula of –3.9% and the right posterior insula of –6.3%. Comparison of conditions D and B revealed values of –4.8% for the posterior insula and –2.0% for the right posterior insula. Compared with baseline, the values were –5.9% for the left posterior insula and –2.8% for the right posterior insula.

Furthermore, subtraction analysis demonstrated a relative deactivation (less activation) of middle temporal/medial superior temporal areas (V5) under conditions in which CV was induced (C and D) compared with the condition in which randomly moving stimuli were presented (B) (Tables 3 and 4). The mean relative decreases of rCBF were –4.7% for left V5 and –5.6% for right V5 when comparing conditions C and B. A comparison of conditions D and B showed relative decreases of –5.1% in left V5 and of –4.1% in right V5. However, when compared with the baseline condition A, C showed an increase in rCBF of +6.9% for left V5 and of +3.7% for right V5. The corresponding values for a comparison of conditions D and A were +2.9% (left V5) and +4.2% (right V5).

Comparison of conditions C and B revealed additional relative rCBF decreases in the left parahippocampal gyrus, the right thalamus, the occipital cortex (BA 18) and areas in the right temporal cortex (Fig. 2 and Table 3). Areas not directly processing visual or vestibular information which showed a decrease with a *Z*-score of >3 were located in the anterior cingulate (right BA 32, with $Z = 3.66$ at $x, y, z = -19, 32, -9$) and in the frontal cortex (right BA 2, with $Z = 3.48$ at $x, y, z = -44, -26, 52$, and right BA 10, with $Z = 3.33$ at $x, y, z = -15, 53, -9$). Similar to the comparison of conditions C and B, a comparison of the conditions D and B revealed a relatively low rCBF increase in an occipital area located at BA 18 (this decrease was also only relative to the non-CV condition where the dots moved randomly, but was not present under the background condition) (Table 4).

Parts of the orbitofrontal cortex, the anterior temporal pole and the cerebellum were excluded from the analyses because they were not in the field of view in all studies.

Pearson's linear correlation on a pixel-wise basis revealed a significant, positive correlation between the perceived intensity of CV and neuronal activity, inducing relative rCBF changes in parietal and occipital areas under both conditions C and D (Tables 5 and 6). The location of the area showing the strongest correlation thus reflects exactly the area determined by the statistical subtraction analysis comparing conditions C and D with B (Fig. 3). An additional area showing a positive correlation just above the significance threshold was located in the rostral part of the anterior cingulate. Significant negative correlations between the perceived intensity of CV and neuronal activity were not observed. Furthermore, there was only a loose, non-significant, negative correlation between the rCBF decreases in the insulae. The tightest negative correlation observed was between the activity in the parieto-occipital cortex and that in the right insula in condition D; the correlation coefficient was $r = -0.68$.

Discussion

Cortical correlates of visually induced self-motion

Two findings of our PET activation study seem most relevant for functional interpretation of the neuronal mechanisms

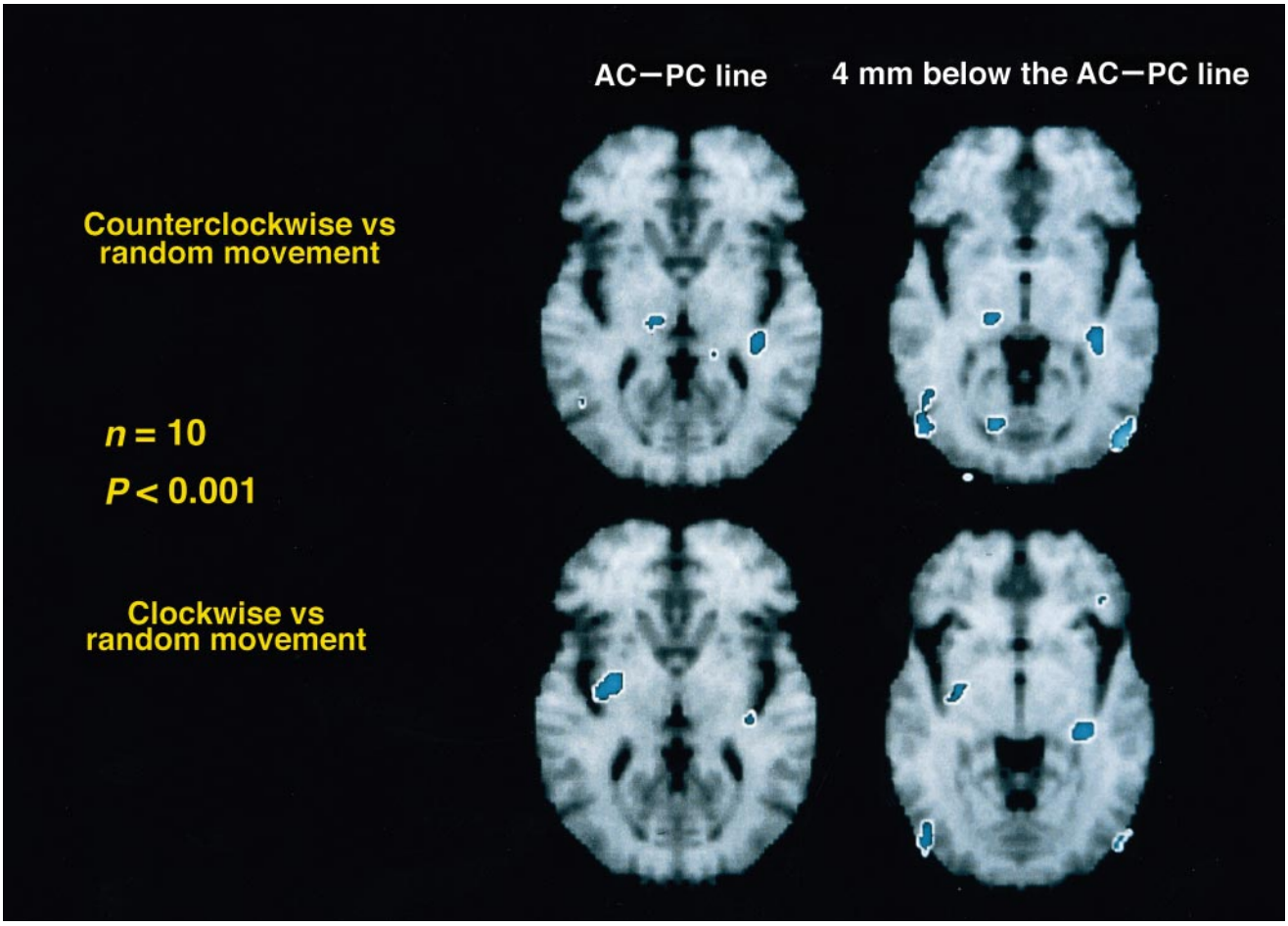

Fig. 2 Comparison of the relative rCBF decreases under both conditions (C and D) that induce CV (clockwise and counter-clockwise, respectively) with the control condition (B) (random movement). All voxels with significant flow (above the statistical threshold of $P < 0.001$, corrected for multiple comparisons) are shown. The transverse images illustrate deactivation of the posterior insula and of V5 (this deactivation is only relative to the control condition; there is an increase in rCBF compared with baseline) .

Table 5 *Talairach coordinates, in each area, of the voxel which shows the maximum significant positive correlation with the perceived intensity of CV under condition C (clockwise CV)*

Area	*x*	*y*	*z*	Correlation coefficient	*Z*-score	*P*-value
BA 31, right posterior cingulate	–3	–35	38	0.74	2.41	<0.05
BA 18/19, left occipital	8	–78	11	0.73	2.32	<0.05

Table 6 *Talairach coordinates, in each area, of the voxel which shows the maximum significant positive correlation with the perceived intensity of CV under condition D (counter-clockwise CV)*

Area	*x*	*y*	*z*	Correlation coefficient	*Z*-score	*P*-value
BA 7/18/19/31, left parieto-occipital	6	–76	29	0.82	2.96	<0.01
BA 32, left anterior cingulate	3	46	4	0.70	2.21	<0.05

subserving visual–vestibular interaction during visually induced apparent self-motion (CV): (i) the bilateral activation of the (non-vestibular) medial parieto-occipital cortex and (ii) the significant concurrent bilateral deactivation of the deep posterior insula, the parieto-insular vestibular cortex.

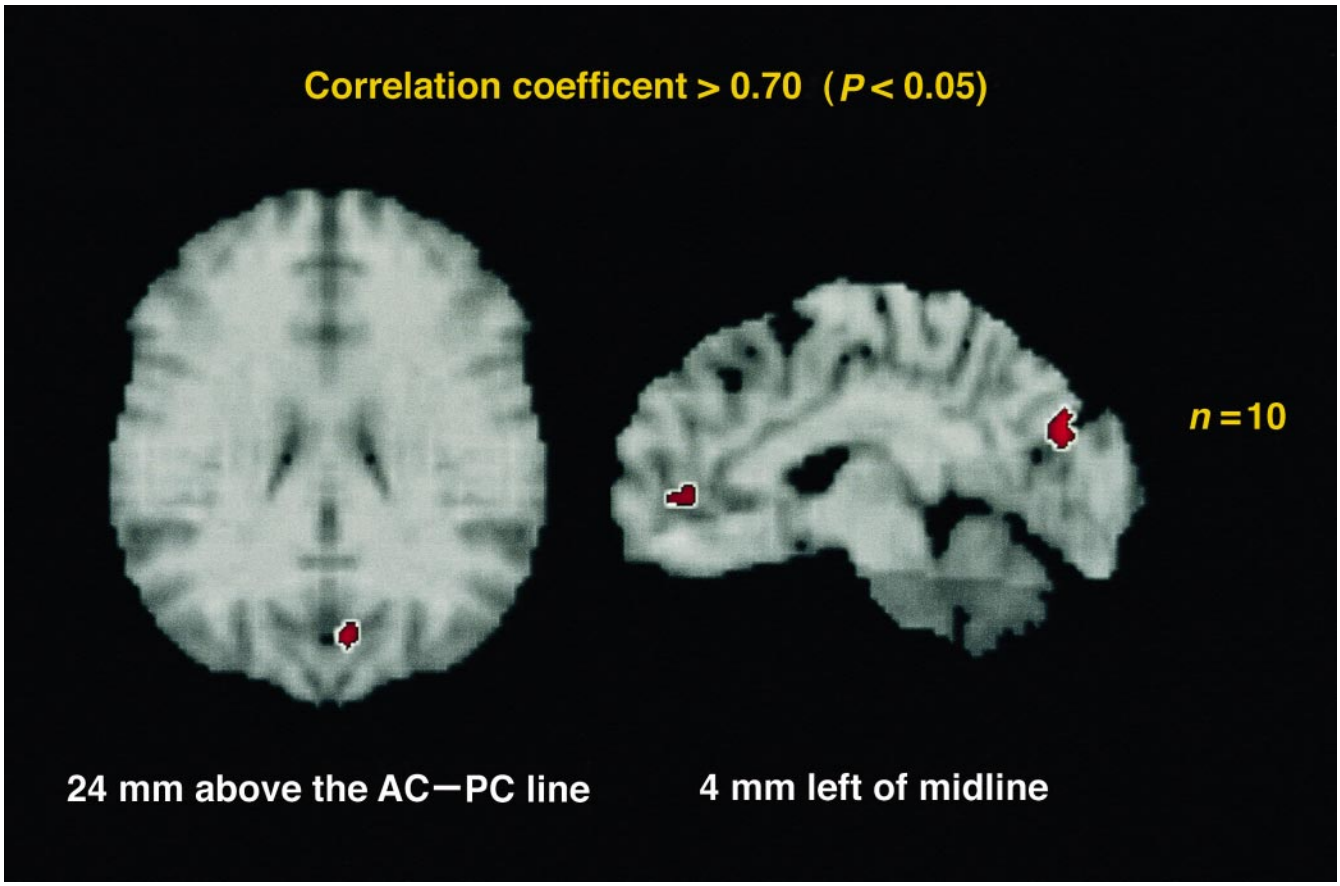

Fig. 3 Correlation analysis illustrating the voxels which have significant positive correlations ($P < 0.05$ after Fisher's transformation from r to Z) with the perceived intensity of CV under condition D (counter-clockwise CV). All voxels with significant correlations are displayed. There is a positive correlation with perceived intensity of CV in an area at the border between occipital and parietal cortex and in the rostral anterior cingulate.

Activation and deactivation of visual association areas

The activation of the medial parieto-occipital cortex, separately from the well-known motion-sensitive middle temporal/medial superior temporal areas, might be a positive (activated) correlate of CV. A significant positive correlation was shown between the perceived intensity of CV and the relative rCBF increases in this area. It is not considered part of the vestibular cortex and is not activated by vestibular caloric stimulation (Bottini *et al*., 1994; Dieterich *et al*., 1996). It corresponds best to a visual area in the parieto-occipital fissure, which was activated in a PET study when the observation of a moving random dot was compared with that of a stationary dot pattern (Dupont *et al*., 1994). This activation in human parieto-occipital cortex was in accordance with that of ventral intraparietal (Colby *et al*., 1993) or parieto-occipital visual areas in monkeys (Galletti *et al*., 1991), in which neurons can be driven by small moving stimuli such as small dots and slits. Care must be taken not to interpret activation of this area simply as the correlate of CV, since the CV-stimulus pattern and the control pattern also differ with respect to coherent versus incoherent visual motion stimulation . Theoretically, activation could be related to the change from random to coherent motion displays. A control condition with coherent visual motion stimulation but no CV would be suitable for clarifying this question. Recent PET studies (Cheng *et al*. 1995; Van Oostende *et al*. 1997; Dupont *et al*. 1997) suggest that the cuneus and precuneus could be involved in extracting directionally coherent motion signals from dynamic dot displays. This lateral occipital area (termed kinetic occipital, with average Talairach coordinates, 31, –91, –2) is located ~20 mm behind the human middle temporal area/V5 (Dupont *et al*. 1997), which is clearly separate from the medial parieto-occipital area (average Talairach coordinates, 1, –75, 25) which was activated in the CV condition in our study. The kinetic occipital area is also separate from the lateral occipital area that showed relative deactivation (average Talairach coordinates, 48, –78, –4) in our study. It should be noted that random displays appear to move more slowly than do coherent displays, and such perceptual differences might contribute to the pattern of activation. Furthermore, another PET study on two representational modes of visual attention has presented evidence that this parieto-occipital area is involved in the control of both within-space and within-object attention (Fink *et al*., 1997).

The only PET study, so far, which has demonstrated cortical activation during visually induced apparent motion is that of de Jong *et al*. (1994); an optical flow stimulus simulated forward motion in depth over a flat surface. They described three main areas of activation associated with optical flow: the dorsal cuneus (V3), the lateroposterior precuneus (or superior parietal lobe) in the right hemisphere and the occipitotemporal ventral surface in the region of the fusiform gyrus in both hemispheres. None of these areas correspond to the medial parieto-occipital area in our study, which lies superior and medial to V3. It must be mentioned that visually induced vection in de Jong's study was apparently forward motion as opposed to roll motion in our study. These authors were interested in the analysis of optical flow as a higher order computation of the visual system rather than in the basic interaction between the visual and the vestibular system for self-motion perception.

The middle temporal/medial superior temporal area was also activated in our CV paradigm but it showed a relative deactivation compared with the response to random dot motion. This area of parieto-occipital deactivation covers V5 according to Zeki *et al*. (1991) which is the transition between BA 19 and BA 37. There are two PET studies of wide-field visual motion stimulation (de Jong *et al*., 1994; Cheng *et al*., 1995) presenting different results with respect to V5. Cheng *et al*. (1995) found activation of the homologue of the middle temporal area and of the inferior parietal lobule. The discrepancy between activation in their study and relative deactivation in our study can simply be explained by the different mode of stimulation; in their study the direction of motion changed each second, a stimulation period which does not induce the sensation of self-motion. Their paradigm, therefore, comes closer to our control condition B with random dot movement than to our CV conditions, and that also resulted in activation of V5.

Deactivation of the vestibular cortex during CV

The area of significant deactivation in the deep posterior insula during CV corresponds to the area activated during caloric vestibular stimulation when measured with similar PET methods (Bottini *et al*., 1994). This area represents the human homologue of parieto-insular vestibular cortex in monkeys (Grüsser *et al*., 1990*a*, *b*). A clinical study on patients with infarctions of the middle cerebral artery territory identified the same area, a lesion of which causes spatial disorientation manifested by significant (mostly contraversive) tilts of perceived vertical (Brandt *et al*., 1994). Among all the known vestibular areas (areas 2v, 3aV, 6 and 7), the parieto-insular vestibular cortex is considered an integration centre for multisensory vestibular function (Grüsser *et al*., 1990*a*, *b*; Brandt *et al*., 1994; Guldin and Grüsser, 1996). It must be assumed that this area dominates the perception of body orientation and self-motion. If this is true, then the question arises as to why this area is deactivated when self-motion is induced by relative motion of the visual scene.

Earlier hypotheses, including our own, on the mechanism of CV emphasized visually induced activation of the vestibular cortex as the neurophysiological correlate required for the transition from perception of object-motion to perception of self-motion (Straube and Brandt, 1987; Grüsser *et al*., 1990*a*, *b*). It was generally accepted that CV is based on visual–vestibular convergence and that the perception of self-motion is mediated by activation of the vestibular cortex (Dichgans and Brandt, 1978; Grüsser *et al*., 1990*a*, *b*). This concept was supported by a series of electrophysiological animal experiments that demonstrated visual–vestibular convergence at the neuronal level in the vestibular nuclei (Dichgans *et al*., 1973), the dorsolateral thalamus (Deecke *et al*., 1974), and vestibular cortex areas such as area 2v (Büttner and Buettner, 1978; Büttner and Henn, 1981), area 3aV (Ödkvist *et al*., 1974), area 6 (Guldin and Grüsser, 1996), area 7 (Faugier-Grimaud and Ventre, 1989) and the parieto-insular vestibular cortex (Grüsser *et al*., 1990*a*, *b*). Neurons in the parieto-insular vestibular cortex of the monkey have large binocular receptive fields, and directional responses have been found to respond equally to body acceleration in one direction and optokinetic stimulation in the opposite direction (Grüsser *et al*., 1990*a*, *b*). It is well known from psychophysical studies in humans that visually induced CV requires large-field stimulation (Brandt *et al*., 1973). Thus, it seemed logical that adequate large-field visual motion stimulation would cause visual information to enter the vestibular system so as to permit the perceptional interpretation of self-motion relative to the surroundings. However, the paradigms in most of the above-cited animal experiments were inadequate to induce CV. Visual–vestibular convergence in the vestibular cortex cannot be automatically related to the perception of self-motion; it may simply reflect the multisensory structure of the different vestibular cortical areas. A 'primary' vestibular cortex does not exist; all vestibular cortex areas are multisensory. Natural vestibular stimulation during locomotion invariably involves concurrent stimulation of the somatosensory (cervical) and visual afferents.

Theoretically, the torsional nystagmus under stimulus conditions C and D might have contributed to the activation pattern. Torsional nystagmus under these conditions was small and irregular, and (most importantly) optokinetic nystagmus has been demonstrated to activate rather than deactivate the posterior insula (Bucher *et al*., 1997; Dieterich *et al*., 1998).

Reciprocal inhibitory visual–vestibular interaction: a sensorimotor mechanism that protects the perception of self-motion from interfering sensory stimuli

Depending on the mode of stimulation, perception of self-motion is dominated by either vestibular input (head

acceleration) or visual input (constant velocity CV), or both. Quantitative visual–vestibular interaction is not simple but complex depending not only on the pattern of visual motion stimulation but also on active postural and locomotor tasks. Reciprocal inhibitory visual–vestibular interaction provides a powerful way to shift the dominant sensorial weight from one modality to the other. As a functional consequence, the concurrent deactivation of the vestibular cortex during CV should decrease the vestibular system's sensitivity to head acceleration. This would make the perception of visually induced CV more robust and largely insensitive to visual–vestibular mismatches occurring during involuntary head accelerations, e.g. in planes or directions different from the main direction of locomotion or transportation. The horizontal direction and speed perceived during constant velocity of car motion are transduced only by the visual system. Concurrent vertical vestibular stimulation caused by involuntary head movements provide vestibular information that is inadequate or even misleading with respect to the perception of self-motion. It is desirable that they be suppressed by deactivation of the vestibular system. The latter hypothesis is supported by earlier findings of significantly increased thresholds for detecting body accelerations (vestibular system) during CV induced by visual motion (visual system) in a combined rotatory chair–drum system (Probst *et al*., 1985). In the light of these considerations an earlier observation can be interpreted as the vestibulo–visual pendant for the perception of self-motion. In a PET study using caloric vestibular irrigation, activation of the vestibular cortex significantly decreased rCBF in the occipital visual cortex covering bilateral BAs 17, 18 and 19 (Wenzel *et al*., 1996). This led us to surmise that deactivation of the visual cortex is beneficial to the organism during vestibular stimulation, since it suppresses visual motion input (e.g. distressing oscillopsia, owing to the retinal slip of the visual scene during vestibular nystagmus). In the same way that deactivation of the visual cortex largely protects the vestibular system from conflicting visual motion input, deactivation of the vestibular cortex prevents visually induced CV from conflicting with vestibular input. Besides this reciprocal inhibitory interaction, it is very likely that visual and vestibular cortices have other forms of interaction depending on actual stimulation, required dynamic spatial orientation and the intended motor tasks. Activation of both cortices is required for adequate perception of self-motion and for postural control in stimulus situations with unexpected, multidirectional transitions between body acceleration and motion at constant velocity.

Acknowledgements

We wish to thank our radiochemistry group and the cyclotron staff for their reliable supply of radiopharmaceuticals and Mrs S. Fürst, Mrs C. Kolligs and Mrs A. Kniehase for their technical assistance, also Mr M. Schönauer for writing the programs for the optokinetic stimulation and Ms J. Benson for copy-editing the manuscript ready for submission. We also wish to thank Dr S. Minoshima, University of Michigan, for his advice and for generously providing us with his statististical parametric mapping software. This work was supported by the Wilhelm-Sander-Stiftung and the Deutsche Forschungsgemeinschaft.

References

Bartenstein P, Weindl A, Spiegel S, Boecker H, Wenzel R, Caballos-Baumann A, *et al*. Central motor processing in Huntington's disease: a positron emission tomography study. Brain 1997; 120: 1553–67.

Bottini G, Sterzi R, Paulesu E, Vallar G, Cappa SF, Erminio F, et al. Identification of the central vestibular projections in man: a positron emission tomography activation study. Exp Brain Res 1994; 99: 164–9.

Brandt Th, Dichgans J, König E. Differential effects of central versus peripheral vision on egocentric and exocentric motion perception. Exp Brain Res 1973; 16: 476–91.

Brandt Th, Dieterich M, Danek A. Vestibular cortex lesions affect the perception of verticality. Ann Neurol 1994; 35: 403–12.

Bucher SF, Dieterich M, Seelos KC, Brandt Th. Sensorimotor cerebral activation during optokinetic nystagmus. Neurology 1997; 49: 1370–7.

Büttner U, Buettner UW. Parietal cortex (2v) neuronal activity in the alert monkey during natural vestibular and optokinetic stimulation. Brain Res 1978; 153: 392–7.

Büttner U, Henn V. Circularvection: psychophysics and single-unit recordings in the monkey. Ann NY Acad Sci 1981; 374: 274–83.

Cheng K, Fujita H, Kanno I, Miura S, Tanaka K. Human cortical regions activated by wide-field visual motion: an H2(15)0 PET study. J Neurophysiol 1995; 74: 413–27.

Colby CL, Duhamel JR, Goldberg ME. Ventral intraparietal areas of the macaque: anatomic location and visual response properties. J Neurophysiol 1993; 69: 902–14.

Deecke L, Schwarz DW, Fredrickson JM. Nucleus ventroposterior inferior (VPI) as the vestibular thalamic relay in the rhesus monkey. I. Field potential investigation. Exp Brain Res 1974; 20: 88–100.

de Jong BM, Shipp S, Skidmore B, Frackowiak RS, Zeki S. The cerebral activity related to the visual perception of forward motion in depth. Brain 1994; 117: 1039–54.

Dichgans J, Brandt Th. Visual-vestibular interaction: effects on self-motion perception and postural control. In: Held R, Leibowitz HW, Teuber HL, editors. Handbook of sensory physiology, Vol. 8. Berlin: Springer; 1978. p. 755–804.

Dichgans J, Schmidt CL, Graf W. Visual input improves the speedometer function of the vestibular nuclei in the goldfish. Exp Brain Res 1973; 18: 319–22.

Dieterich M, Brandt Th, Bartenstein P, Wenzel R, Danek A, Lutz S, et al. Different vestibular cortex areas activated during caloric irrigation: A PET study [abstract]. J Neurol 1996; 243 Suppl 2: S40.

Dieterich M, Bucher SF, Seelos KC, Brandt Th. Horizontal or vertical optokinetic stimulation activates visual motion-sensitive,

ocular motor and vestibular cortex areas with right hemispheric dominance. An FMRI study. Brain 1998; 121:

Dupont P, Orban GA, De Bruyn B, Verbruggen A, Mortelmans L. Many areas in the human brain respond to visual motion. J Neurophysiol 1994; 72: 1420–4.

Dupont P, De Bruyn B, Vandenberghe R, Rosier AM, Michiels I, Marchal G, et al. The kinetic occipital region in human visual cortex. Cereb Cortex 1997; 7: 283–92.

Faugier-Grimaud S, Ventre J. Anatomic connections of inferior parietal cortex (area 7) with subcortical structures related to vestibulo-ocular function in a monkey (Macaca fascicularis). J Comp Neurol 1989; 280: 1–14.

Fink GR, Dolan RJ, Halligan PW, Marshall JC, Frith CD. Within-space and within-object attention: shared and specific neural mechanisms. Neuroimage 1997; 5 (4 Pt 2): 90.

Fox PT, Raichle ME. Stimulus rate dependence of regional cerebral blood flow in human striate cortex, demonstrated by positron emission tomography. J Neurophysiol 1984; 51: 1109–20.

Friston KJ, Frith CD, Liddle PF, Frackowiak RS. Comparing functional (PET) images: the assessment of significant change. J Cereb Blood Flow Metab 1991; 11: 690–9.

Galletti C, Battaglini PP, Fattori P. Functional properties of neurons in the anterior bank of the parieto-occipital sulcus of the macaque monkey. Eur J Neurosci 1991; 3: 452–61.

Grüsser OJ, Pause M, Schreiter U. Localization and responses of neurones in the parieto-insular vestibular cortex of awake monkeys (Macaca fascicularis). J Physiol (Lond) 1990a; 430: 537–57.

Grüsser OJ, Pause M, Schreiter U. Vestibular neurones in the parieto-insular cortex of monkeys (Macaca fascicularis): visual and neck receptor responses. J Physiol (Lond) 1990b; 430: 559–83.

Guldin W, Grüsser OJ. The anatomy of the vestibular cortices of primates. In: Collard M, Jeannerod M, Christen Y, editors. Le cortex vestibulaire. Boulogne: Ipsen; 1996. p. 18–26.

Kosslyn SM, Alpert NM, Thompson WL, Chabris CF, Rauch SL, Anderson AK. Identifying objects seen from different viewpoints. A PET investigation. Brain 1994; 117: 1055–71.

Minoshima S, Koeppe RA, Mintun MA, Berger KL, Taylor SF, Frey KA, et al. Automated detection of the intercommissural line for stereotactic localization of functional brain images. J Nucl Med 1993; 34: 322–9.

Minoshima S, Koeppe RA, Frey KA, Kuhl DE. Anatomic standardization: linear scaling and nonlinear warping of functional brain images. J Nucl Med 1994; 35: 1528–37.

Ödkvist LM, Schwarz DW, Fredrickson JM, Hassler R. Projection of the vestibular nerve to the area 3a arm field in the squirrel monkey (Saimiri sciureus). Exp Brain Res 1974; 21: 97–105.

Probst Th, Straube A, Bles W. Differential effects of ambivalent visual-vestibular-somatosensory stimulation on the perception of self-motion. Behav Brain Res 1985; 16: 71–9.

Straube A, Brandt Th. Importance of the visual and vestibular cortex for self-motion perception in man (circularvection). Hum Neurobiol 1987; 6: 211–8.

Talairach J, Tournoux P. Co-planar stereotaxic atlas of the human brain. Stuttgart: Thieme; 1988.

Van Oostende S, Sunaert S, Van Hecke P, Marchal G, Orban GA. The kinetic occipital (KO) region in man: an fMRI study. Cereb Cortex 1997; 7: 690–701.

Wenzel R, Bartenstein P, Dieterich M, Danek A, Weindl A, Minoshima S, et al. Deactivation of human visual cortex during involuntary ocular oscillations: a PET activation study. Brain 1996; 119: 101–10.

Worsley KJ, Evans AC, Marrett S, Neelin P. A three-dimensional statistical analysis for CBF activation studies in human brain [see comments]. J Cereb Blood Flow Metab 1992; 12: 900–18. Comment in: J Cereb Blood Flow Metab 1993; 13: 1040–2.

Zeki S, Watson JD, Lueck CJ, Friston KJ, Kennard C, Frackowiak RS. A direct demonstration of functional specialization in human visual cortex. J Neurosci 1991; 11: 641–9.

Received January 6, 1998. Revised March 23, 1998.
Accepted April 4, 1998